

# The nature of the variable millimetre–selected AGN in the Brightest Cluster Galaxy of Abell 851

R. A. Cheale,<sup>1</sup><sup>\*</sup> J. E. Geach,<sup>1</sup> A. C. Edge,<sup>2</sup> Y. C. Perrott,<sup>3</sup> T. Cantwell<sup>4</sup>

<sup>1</sup>Center for Astrophysics Research, School of Physics, Astronomy & Mathematics, University of Hertfordshire, Hatfield, AL10 9AB

<sup>2</sup>Centre for Extragalactic Astronomy, Department of Physics, Durham University, South Road, Durham, DH1 3LE

<sup>3</sup>Astrophysics Group, Cavendish Laboratory, 19 J. J. Thomson Avenue, Cambridge CB3 0HE

<sup>4</sup>Jodrell Bank Centre for Astrophysics, Alan Turing Building, School of Physics and Astronomy, University of Manchester, M13 9PL

Accepted XXX. Received YYY; in original form ZZZ

## ABSTRACT

We present the detection of a bright 3 mm continuum source in the Brightest Cluster Galaxy (BCG) in Abell 0851 ( $z = 0.411$ ) with the Northern Extended Millimeter Array (NOEMA). When this detection is compared to other multi-frequency observations across 21cm–100 $\mu$ m, including new Arcminute Microkelvin Imager 15 GHz observations, we find evidence for a relatively flat, variable core source associated with the BCG. The radio power and amplitude of variability observed in this galaxy is consistent with the cores in lower redshift BCGs in X-ray–selected clusters, and the flat mm–cm spectrum is suggestive of the BCG being a low luminosity AGN archetype. The discovery of this system could provide a basis for a long-term study of the role of low luminosity radio mode ‘regulatory’ feedback in massive clusters.

**Key words:** galaxies: clusters: individual: Abell 851 – galaxies:clusters:individual (A851, Cl 0939+4713) – galaxies:evolution – galaxies: elliptical and lenticular, cD – techniques: interferometric

## 1 INTRODUCTION

The discovery that every massive galaxy contains a super-massive black hole (SMBH), and that the masses of the stellar bulge and SMBH are correlated (Magorrian et al. 1998; Silk & Rees 1998) demonstrates that the growth of the central black hole and its host galaxy are inexorably linked. Black hole accretion releases large amounts of feedback energy and momentum into the interstellar medium (and beyond) via collimated jets and fast winds driven from the hot accretion disc, and is thought to be a driving feature in the regulation of stellar mass growth (Bower et al. 2006; Croton et al. 2006). Active Galactic Nucleus (AGN) feedback is now an established feature of galaxy formation models that are required to correctly reproduce the key observable features of the local galaxy population (e.g., Sijacki et al. 2007; Booth & Schaye 2009; Fabian 2012; Ishibashi & Fabian 2012).

We observe a wide range of nuclear activity in galaxies; from low luminosity or quiescent systems such as Sgr A<sup>\*</sup> at the center of the Milky Way, up to powerful radio galaxies and quasars where AGN feedback can expel large fractions of the gas reservoir and pump energy into the circumgalactic and intergalactic medium (Gaspari et al. 2011; Dubois et al. 2013; Schaye et al. 2015). This substantial energy input into

the local environment is necessary for regulating stellar mass growth on galaxy scales by stifling the cooling of intracluster gas (see; Fabian 2012), but this must be sustained for many Gyr to maintain the suppression of stellar mass growth in the host galaxy (Dunn & Fabian 2008). It is likely that a self-regulating process affects the growth of the central black hole, as exhibited in numerical simulations (e.g., Springel et al. 2005) and galaxy formation theories (Silk & Rees 1998; Benson 2010).

Variability is associated with all AGN from high luminosity quasars to Seyfert galaxies (McHardy et al. 2006). Low-luminosity AGN (LLAGN), like Sgr A<sup>\*</sup>, M81 (Sakamoto et al. 2001; Schodel et al. 2007), Centaurus A (Israel et al. 2008) and, NGC7469 (Baldi et al. 2015) have relatively low Eddington rates ( $L \approx 0.1 L_{\text{Edd}}$ ) and often exhibit bright inverted/flat cm–mm spectra likely originating from a compact core (e.g. Behar et al. 2018). Recent advances in mm–interferometry in resolution and sensitivity make the detection of such LLAGN more probable. Indeed, work by Doi et al. 2011 supports the view that many large passive galaxies have compact millimetre cores with significant variable radio activity at their cores, but few systematic searches for such LLAGN have yet been made, and in general the detection and monitoring of AGN variability requires multiple observations over weeks to decades.

Here we present evidence of a variable AGN in the well

<sup>\*</sup> E-mail: r.cheale@herts.ac.uk (RAC)

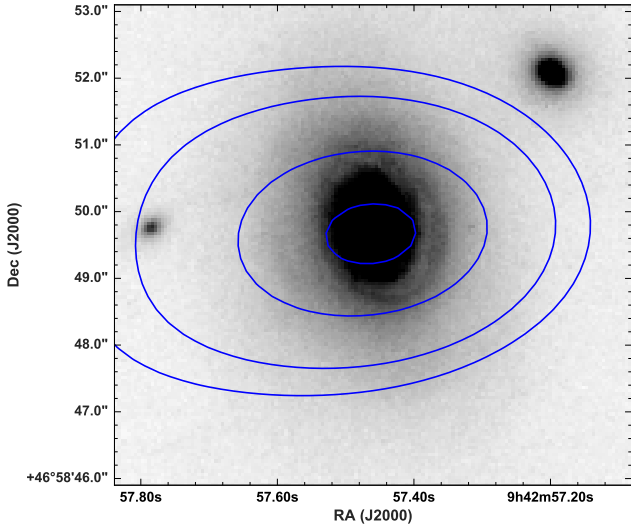


**Figure 1.** The archival *HST*/ACS F814W filter optical imaging. DG92-311 is located  $\alpha$ ;  $09^{\text{h}} 42^{\text{m}} 57.50^{\text{s}}$ ,  $\delta$ ;  $46^{\text{d}} 48^{\text{m}} 50.00^{\text{s}}$ . The primary beam corrected significance contours are overlaid, initiating at  $1.05 \text{ mJy}$  ( $3\sigma$ ) and increasing in  $1\sigma$  intervals. We find a corrected (see Section 2.2) peak flux density of  $S_{3.6\text{mm}} 1.59 \pm 0.15 \text{ mJy}$ .

known cluster Abell 851 (also known as CL 0939+4713), a rich (Seitz et al. 1996) cluster ( $M \sim 10^{14} M_{\odot}$  at  $z = 0.411$ ) containing several hundred spectroscopically classified members (Dressler & Gunn 1992). The galaxy in question is a possible Sa/S0 transition object close to the cluster centre, catalogued by Dressler & Gunn (1992) as object 311 and hence referred to in this paper as DG92-311. DG92-311 is optically classified as an early-type disc (Sa/S0) with post-starburst spectral features; namely weak nebular emission but relatively strong Balmer absorption ((k+a) Belloni et al. 1995; Dressler et al. 1999; Oemler Jr et al. 2009). In this Letter we present the observational evidence across the radio-far-infrared spectral energy distribution of DG92-311, including new 3 mm IRAM Plateau de Bure interferometer and new 1.9 cm Arcminute Microkelvin Imager observations. Throughout we assume a  $\Lambda$ CDM cosmology with  $H_0 = 67.3 \text{ km s}^{-1} \text{ Mpc}^{-1}$ ,  $\Omega_{\text{M}} = 0.315$ , and  $\Omega_{\Lambda} = 0.685$  (Planck Collaboration et al. 2016).

## 2 DATA COLLECTION AND ANALYSIS

We make use of a number of archival observations of DG92-311 including *WISE* 3.4 –  $22\mu\text{m}$ , *Herschel* PACS and SPIRE 100– $500\mu\text{m}$ , James Clerk Maxwell Telescope (JCMT) SCUBA  $850\mu\text{m}$  (project M00BH05), BIMA 1.05 cm, AMI 1.9 cm and, VLA/FIRST 6.2 – 21 cm band archives. The *HST*/ACS F814W filter optical imaging is shown in Figure 1 (data retrieved from the MAST archive HST, project 10418). We report the various flux density measurements of DG92-311 in Table 1.

### 2.1 Archival Data

#### 2.1.1 JCMT/SCUBA

Observations of DG92-311 by SCUBA at  $850\mu\text{m}$  were conducted on the 27th November 2000. The target was observed in the ‘jiggle’ map mode used for observing sources smaller than the array (Jenness et al. 2000). The target is formally undetected in the archival map, and so we determine an upper limit by sampling a large number of random pixels around the source position and fit a Gaussian to the resulting pixel distribution. We take the standard deviation of the Gaussian as a measure of the  $1\sigma$  noise, and determine a  $3\sigma$  upper limit of  $S_{850\mu\text{m}} < 4.6 \text{ mJy}$  for DG92-311.

#### 2.1.2 Herschel Lensing Survey

The *Herschel* Lensing Survey (HLS Egami et al. 2010) observed Abell 851 with the PACS (100 and  $160\mu\text{m}$ ) and SPIRE (250, 350 and  $500\mu\text{m}$ ) instruments. These far-IR/sub-mm bands are useful to constrain the peak of the thermal dust emission. Rawle et al. (2012) analyse a number of BCGs from the HLS including A851. Photometry in the SPIRE bands was reduced by using the IRAF package ALLSTAR (Tody 1993) by fitting the Point Spread Function to source locations. In the PACS bands fluxes were measured by using aperture photometry with the use of SEXTRACTOR (Bertin & Arnouts 1996); methods are described in detail in Rawle et al.. DG92-311 was detected in all but the  $500\mu\text{m}$  band, and we report the measurements in Table 1.

### 2.2 NOEMA observations

In project S14BV (PI: Geach), we observed DG92-311 as part of a larger 3 mm mosaic of Abell 851 to search for CO(2–1) emission associated with cluster members (e.g. Geach et al. 2009). Abell 851 was observed in configuration D (baseline separations up to 150 m) for maximum sensitivity. We adopted a similar set up to Geach et al. (2009), where the 3 mm receiver was set to the frequency of the redshifted CO(1–0) line at the redshift of the cluster, and the correlator was set up with 2.5-MHz spacing ( $2 \times 64$  channels, 320-MHz bandwidth). The data were reduced using the standard Grenoble Image and Line Data Analysis Software (GILDAS<sup>1</sup>) and converted to a UVFITS data table for imaging in the CASA environment (McMullin et al. 2007). The 3 mm continuum detection became obvious in a channel-by-channel inspection of the data cube. We note the source lies close to the edge of the  $50''$  primary beam, and we apply an appropriate primary beam correction to measure a flux density  $S_{3.6\text{mm}} = 2.6 \pm 0.4 \text{ mJy}$ . The 3 mm contours are overlaid on *HST*/ACS optical imaging in Figure 1.

### 2.3 The Arcminute Microkelvin Imager

The Arcminute Microkelvin Imager (AMI; Zwart et al. 2008; Hickish et al. 2018) is a dual aperture-synthesis array that operates between 13.9 – 18.2 GHz with 2048 channels. The principle use of the AMI detector is for imaging the Sunyaev-Zel’dovich effect by observing galaxy clusters. However, we

<sup>1</sup> <http://www.iram.fr/IRAMFR/GILDAS>

make use of the instrument for its favourable bandwidth for observations pointed at A851. DG92-311 was observed by AMI on the 4<sup>th</sup> October 2017 with an integration time of 7200s, we make use of AMI-LA with angular resolution of 30'' using seven of the eight 12.8 m diameter dishes.

The AMI-LA data were calibrated and imaged in CASA. Primary calibration was performed using a nearby observation of 3C 286, using the Perley & Butler 2013a flux density scale along with a correction for the fact that AMI measures I+Q, using the polarization fraction and angle fits from Perley & Butler 2013b; this is an  $\approx 4.5\%$  correction for 3C 286 over the AMI band. The primary calibration observation supplied an instrumental bandpass in both phase and amplitude. This was applied to the target data, as well as a correction for atmospheric amplitude variations produced by the ‘rain gauge’, which is a noise injection system used to measure the atmospheric noise contribution (see; Zwart et al. 2008). The nearby bright point source 5C 5.175 was observed throughout the observation in an interleaved manner and was used to correct for atmospheric and/or instrumental phase drift. After narrow-band RFI flagging, the data were binned down to 64 channels to reduce processing time and imaged at the central frequency, 15.5 GHz. We used the ‘clean’ task, using multi-frequency synthesis with nterms=2 which allows for a frequency dependence of the sky brightness. We used the CASA graphical Gaussian fitting task on the resulting image to confirm that the source was unresolved and measure a peak flux density of signal of  $S_{1.9\text{cm}} = 3.46 \pm 0.09\text{mJy}$  including thermal noise and a 5% systematic error estimate at 15.5GHz (1.9cm). Hurley-Walker et al. 2012 (HW12) also observed cluster A851 in 2012 with AMI-LA reporting  $S_{\text{LA}} = 2.2 \pm 0.1$  at the position of DG92-311 (Table 12, ID B in HW12) we include both results in Table 1.

### 3 ANALYSIS AND DISCUSSION

#### 3.1 Spectral energy distribution

In Figure 2 we construct the spectral energy distribution using the data in Table 1 and fit three components spanning the radio, sub-mm and far-IR bands. Note that, despite the data spanning a range of angular resolutions, all observations are unresolved for DG92-311 and a comparison of the beam sizes to the optical imaging of DG92-311 shows that we are in all cases measuring galaxy-integrated flux densities with negligible contamination from neighbouring or background sources.

The *Herschel* 100 – 350 $\mu\text{m}$  flux measurements allow for a simple least squares fit of an isothermal modified blackbody, where we employ a standard emissivity term,  $\beta = 1.5$  (Hildebrand 1983; Casey 2012), allowing dust temperature as the free parameter. We find a best-fit dust temperature of  $T_D = 24\text{K}$ , consistent with the S0 morphological-temperature results found by Bendo et al. 2003. We also make use of the well known FIR/sub-mm templates described by Dale & Helou 2002 to fit the 100 – 350 $\mu\text{m}$  data. We normalise to the 160 $\mu\text{m}$  PACS detection as it lies near the peak of the thermal emission and we overlay the template which is best suited to the *Herschel* data (correspond-

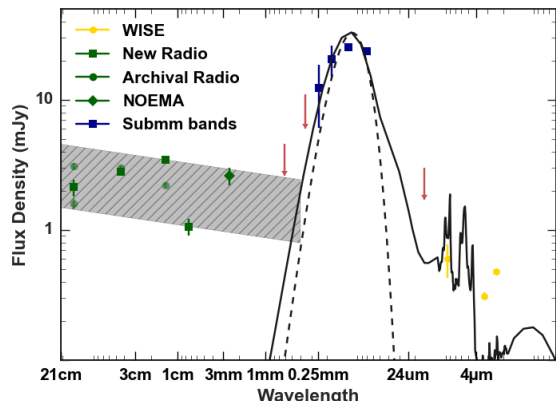


**Figure 2.** The rest-frame spectral energy distribution for DG92-311. The blue squares cover the sub-mm wavebands: 100, 160, 250, 350, 500, 850 $\mu\text{m}$ , the green diamond is the imaged IRAM PdBI 3.6mm detection, the gold hexagons are the FIR WISE bands, green squares are the most recent radio observations whereas the fainter green circles are historic observations (listed in Table 1). The shaded region shows the synchrotron emission amplitude range of a source with  $\alpha \approx -0.1$  over two decades, the black dashed line is thermal blackbody component fit with a characteristic temperature of  $T = 24\text{K}$  and, finally, the black solid line is a SPIRE 250 $\mu\text{m}$  normalised template with  $\alpha = 3.125$  from Dale & Helou 2002

ing to a power law index of  $\alpha = 1.875$ ), as a solid black curve.

In the radio bands the spectral index of the synchrotron power law component is estimated from the ratio of the most recent NOEMA 3 mm and the average AMI 1.9 cm observations, giving  $\alpha \approx -0.1$  for  $S \propto \nu^\alpha$ . We overlay a grey hashed region onto Figure 2 to represent the range of flux normalisations that fit the full range of radio observations up to the Rayleigh-Jeans tail of the thermal dust emission. While it is very likely that the synchrotron component will have some spectral curvature over the three orders of magnitude in frequency plotted Hogan et al. 2015b, as we lack simultaneous observations over the full spectral range then we must interpret any variability assuming a single power law index, as we discuss in the next section.

#### 3.2 Variability

The radio light curves with observations from VLA, BIMA, AMI and NOEMA spanning near two decades in time is shown in Figure 3. The source exhibits a flat spectrum over 1.4–82 GHz range and is unlikely to be extended on the  $>$ few arcsecond scales of the resolution of the majority of observations (Table 1). Although none of these data were taken simultaneously, it is clear that over the 1.4–82 GHz frequency range covered there has been a significant change in the normalisation of the power-law synchrotron component over the past 20–30 years. The source varies at the same frequency and resolution in data from both the VLA at 1.4 GHz and AMI-LA at 15 GHz; furthermore, the NOEMA data has better angular resolution than the BIMA and AMI-LA data but is brighter than all but the most recent AMI-LA point. If flux were being missed on larger scales, then one would expect

**Table 1.** Observed bands for Abell 851, the flux density (S) and uncertainty ( $\delta S$ ) for each wavelength is provided in column 3 and 4.

Instrument	Angular Resolution	Wavelength	S (mJy)	$\delta S$ (mJy)	Reference	Observation Date
WISE	6.1''	3.4 $\mu$ m	0.48	0.02	Wright et al. 2010	2010-2013
WISE	6.4''	4.6 $\mu$ m	0.31	0.02	Wright et al. 2010	2010-2013
WISE	6.5''	12 $\mu$ m	0.60	0.17	Wright et al. 2010	2010-2013
WISE	12''	22 $\mu$ m	< 3.0	—	Wright et al. 2010	2010-2013
PACS	8''	100 $\mu$ m	23.7	0.3	Rawle et al. 2012	2003-07-01
PACS	13''	160 $\mu$ m	25.3	0.7	Rawle et al. 2012	2003-07-01
SPIRE	18''	250 $\mu$ m	20.5	5.5	Rawle et al. 2012	2003-07-01
SPIRE	25''	350 $\mu$ m	12.3	6.2	Rawle et al. 2012	2003-07-01
SPIRE	36''	500 $\mu$ m	<11.0	—	Rawle et al. 2012	2003-07-01
SCUBA	14''	850 $\mu$ m	< 4.6	—	Smail et al. 2002	2000-11-27
IRAM PdBI	6''	3.6 mm	2.59	0.40	This work	2014-06-07
BIMA	23''	1.05 cm	1.06	0.15	Coble et al. 2007	1997-07-15
AMI-LA	30''	1.9cm	2.2	0.1	Hurley-Walker et al. 2012	2008-2009
AMI-LA	30''	1.9cm	3.46	0.09	This work	2017-10-04
VLA	4''	6.2 cm	3.01	0.14	Archive <sup>3</sup>	1990-12-01
VLA	4''	6.2 cm	2.79	0.03	Archive <sup>3</sup>	1993-08-28
VLA	4''	21 cm	1.6	0.16	Morrison 1999	1996-01-06
VLA/FIRST	4''	21 cm	2.13	0.31	White et al. 1997	1997-03-25
VLA	4''	21 cm	3.1	0.2	Condon et al. 1990	1987-05-23

the 3 mm point to be fainter. The source appears to have been at a minimum around the year 2000 and has gradually increased in brightness by a factor of more than three in the past 18 years. We argue that the observed radio variability is intrinsic to the source.

This magnitude and timescale for radio variability is observed in local BCGs such as NGC1275 in the Perseus cluster (Dutson et al. 2014) and a sample of bright, flat spectrum cores monitored with the OVRO 40m (Hogan et al. 2015b). All of these variable BCGs are found in dusty BCGs with luminous optical lines in cool core clusters (Hogan et al. 2015b) with no evidence for jet contribution. As can be seen from the *HST* optical imaging in Figure 1, DG92-311 does exhibit dust lanes and the bright sub-mm detections across the *Herschel* bands indicate the presence of dust in the interstellar medium. DG92-311 does not exhibit any significant  $H\alpha$  line emission (Koyama et al. 2011) and, although there is no *Chandra* observation of A851 and DG92-311 falls on a chip-gap of the EPIC camera in the only on-axis pointing with *XMM-Newton*, the wider structure of the cluster in the X-ray from ROSAT (Schindler et al. 1998) suggests that any cool core in A851 is weak. On this basis DG92-311 is atypical of BCGs with a strong radio core. The observed radio power of DG92-311 of  $\approx 10^{24}$  W Hz<sup>-1</sup> implies that it falls in the upper quartile of core radio power of all X-ray luminous clusters (Hogan et al. 2015a) with a cool core or in the uppermost 3% of core radio power for BCGs without a surrounding cool core. While the observed radio variability could be due to a jet, the similarity in its amplitude and time-scale implies a similar origin for the core emission in other BCGs. Therefore DG92-311 is an important system that may have an unusual X-ray environment, and therefore more detailed X-ray follow-up is required to determine the properties of the intracluster gas on scales of 10s kpc around the BCG.

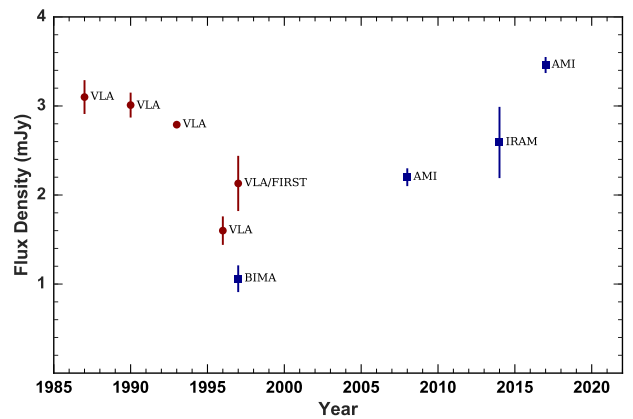


**Figure 3.** Two decades of radio data from VLA, BIMA, AMI and IRAM reveals an up-turn in the BCG light curve. We derive out spectral index from the most recent observations by AMI and IRAM-PdBI. Red squares indicate data  $\geq 10$  GHz and blue circles  $< 10$  GHz. It is clear from the figure that at  $< 10$  GHz there has been a gradual decline in luminosity but in bands  $\geq 10$  GHz there is evidence of an increase.

## 4 CONCLUSIONS

Optically, DG92-311 appears to be a relatively unremarkable, dusty early-type disc galaxy (Sa/S0) but when observed in the radio–submillimetre this optically inactive galaxy appears to contain a relatively powerful, variable LLAGN in what is the Brightest Cluster Galaxy in a rich cluster. While the variability of a factor of three on decade timescales is consistent with other BCGs, the lack of a prominent cool core in the host cluster is surprising and highlights the need to assess the temporal behaviour of all massive galaxies in cluster cores, particularly in the millimetre wavelengths, to ascertain the underlying level radio mode regulatory feedback in massive clusters.

**ACKNOWLEDGMENTS**

RAC thanks Tim Pearson for useful comments and the anonymous referee for useful discussion. RAC is supported by the Royal Society, JEG is supported by a Royal Society University Research Fellowship. ACE acknowledges support from STFC grant ST/P00541/1. YCP is supported by a Trinity College JRF. This work is based on observations carried out under project number S14BV with the IRAM PdB Interferometer. IRAM is supported by INSU/CNRS (France), MPG (Germany) and IGN (Spain). We thank the staff of the Mullard Radio Astronomy Observatory for their invaluable assistance in the operation of AMI, which is supported by Cambridge University and the STFC. This research has made use of the NASA/IPAC Extragalactic Database (NED) which is operated by the Jet Propulsion Laboratory, California Institute of Technology, under contract with the National Aeronautics and Space Administration.

**REFERENCES**

Baldi R. D., Behar E., Laor A., Horesh A., 2015, *Monthly Notices of the Royal Astronomical Society*, 454, 4277  
 Behar E., Vogel S., Baldi R. D., Smith K. L., Mushotzky R. F., 2018, *Monthly Notices of the Royal Astronomical Society*, 478, 399  
 Belloni P., Bruzual A. G., Thimm G. J., Roser H.-J., 1995, *Astronomy and Astrophysics*, 297, 61  
 Bendo G. J., et al., 2003, *The Astronomical Journal*, 125, 2361  
 Benson A. J., 2010, *Physics Reports*, 495, 33  
 Bertin E., Arnouts S., 1996, *Astronomy and Astrophysics Supplement Series*, 117, 393  
 Booth C. M., Schaye J., 2009, *Monthly Notices of the Royal Astronomical Society*, 398, 53  
 Bower R. G., Benson A. J., Malbon R., Helly J. C., Frenk C. S., Baugh C. M., Cole S., Lacey C. G., 2006, *Monthly Notices of the Royal Astronomical Society*, 370, 645  
 Casey C. M., 2012, *Monthly Notices of the Royal Astronomical Society*, 425, 3094  
 Coble K., et al., 2007, *The Astronomical Journal*, 134, 897  
 Condon J. J., Dickey J. M., Salpeter E. E., 1990, *The Astronomical Journal*, 99, 1071  
 Croton D. J., et al., 2006, *Monthly Notices of the Royal Astronomical Society*, 365, 11  
 Dale D. A., Helou G., 2002, *The Astrophysical Journal*, 576, 159  
 Doi A., Nakanishi K., Nagai H., Kohno K., Kameno S., 2011, *The Astronomical Journal*, 142, 167  
 Dressler A., Gunn J. E., 1992, *The Astrophysical Journal Supplement Series*, 78, 1  
 Dressler A., Smail I., Poggianti B., Butcher H., Couch W., Ellis R., Oemler Jr A., 1999, *The Astrophysical Journal Supplement Series*, 122, 51  
 Dubois Y., Pichon C., Devriendt J., Silk J., Haehnelt M., Kimm T., Slyz A., 2013, *Monthly Notices of the Royal Astronomical Society*, 428, 2885  
 Dunn R. J. H., Fabian A. C., 2008, *Monthly Notices of the Royal Astronomical Society*, 385, 757  
 Dutton K. L., Edge A. C., Hinton J. A., Hogan M. T., Gurwell M. A., Alston W. N., 2014, *Monthly Notices of the Royal Astronomical Society*, 442, 2048  
 Egami E., et al., 2010, *Astronomy and Astrophysics*, 518, L12  
 Fabian A. C., 2012, *Annual Review of Astronomy and Astrophysics*, 50, 455  
 Gaspari M., Brighenti F., D’Ercole A., Melioli C., 2011, *Monthly Notices of the Royal Astronomical Society*, 415, 1549

Hickish J., et al., 2018, *Monthly Notices of the Royal Astronomical Society*, 475, 5677  
 Hildebrand R. H., 1983, *Quarterly Journal of the Royal Astronomical Society*, 24, 267  
 Hogan M. T., et al., 2015a, *Monthly Notices of the Royal Astronomical Society*, 453, 1201  
 Hogan M. T., et al., 2015b, *Monthly Notices of the Royal Astronomical Society*, 453, 1223  
 Hurley-Walker N., et al., 2012, *Monthly Notices of the Royal Astronomical Society*, 419, 2921  
 Ishibashi W., Fabian A. C., 2012, *Monthly Notices of the Royal Astronomical Society*, 427, 2998  
 Israel F. P., Raban D., Booth R. S., Rantakyr   F. T., 2008, *Astronomy and Astrophysics*, 483, 741  
 Jenness T., Lightfoot J. F., Holland W. S., Greaves J. S., Economou F., 2000, *Imaging at Radio through Submillimeter Wavelengths*, 217, 205  
 Koyama Y., Kodama T., Nakata F., Shimasaku K., Okamura S., 2011, *The Astrophysical Journal*, 734, 66  
 Magorrian J., et al., 1998, *The Astronomical Journal*, 115, 2285  
 McHardy I. M., Koerding E., Knigge C., Uttley P., Fender R. P., 2006, *Nature*, 444, 730  
 McMullin J. P., Waters B., Schiebel D., Young W., Golap K., 2007, *Astronomical Data Analysis Software and Systems XVI*, 376, 127  
 Morrison G. E., 1999, Ph.D. Thesis, p. 314  
 Oemler Jr A., Dressler A., Kelson D., Rigby J., Poggianti B. M., Fritz J., Morrison G., Smail I., 2009, *The Astrophysical Journal*, 696, 1063  
 Perley R. A., Butler B. J., 2013a, *The Astrophysical Journal Supplement Series*, 204, 19  
 Perley R. A., Butler B. J., 2013b, *The Astrophysical Journal Supplement Series*, 206, 16  
 Planck Collaboration et al., 2016, *Astronomy and Astrophysics*, 594, A1  
 Rawle T. D., et al., 2012, *The Astrophysical Journal*, 747, 29  
 Sakamoto K., Fukuda H., Wada K., Habe A., 2001, *The Astronomical Journal*, 122, 1319  
 Schaye J., et al., 2015, *Monthly Notices of the Royal Astronomical Society*, 446, 521  
 Schindler S., Belloni P., Ikebe Y., Hattori M., Wambsganss J., Tanaka Y., 1998, *Astronomy and Astrophysics*, 338, 843  
 Schodel R., Krips M., Markoff S., Neri R., Eckart A., 2007, *Astronomy and Astrophysics*, 463, 551  
 Seitz C., Kneib J.-P., Schneider P., Seitz S., 1996, *Astronomy and Astrophysics*, 314, L707  
 Sijacki D., Springel V., Di Matteo T., Hernquist L., 2007, *Monthly Notices of the Royal Astronomical Society*, 380, 877  
 Silk J., Rees M. J., 1998, *Astronomy and Astrophysics*, 331, L1  
 Smail I., Ivison R. J., Blain A. W., Kneib J.-P., 2002, *Monthly Notices of the Royal Astronomical Society*, 331, 495  
 Springel V., Di Matteo T., Hernquist L., 2005, *Monthly Notices of the Royal Astronomical Society*, 361, 776  
 Tody D., 1993, in *IRAF in the Nineties. Astronomical Data Analysis Software and Systems II*, p. 173  
 White R. L., Becker R. H., Helfand D. J., Gregg M. D., 1997, *The Astrophysical Journal*, 475, 479  
 Wright E. L., et al., 2010, *The Astronomical Journal*, 140, 1868  
 Zwart J. T. L., et al., 2008, *Monthly Notices of the Royal Astronomical Society*, 391, 1545

This paper has been typeset from a  $\text{\TeX}/\text{\LaTeX}$  file prepared by the author.